Available online at www.sciencedirect.com

ScienceDirect

Energy Procedia 140 (2017) 423–433

Energy Procedia

www.elsevier.com/locate/procedia

AiCARR 50th International Congress; Beyond NZEB Buildings, 10-11 May 2017, Matera, Italy

# On the optimal mix between lead-acid battery and thermal storage tank for PV and heat pump systems in high performance buildings

Alessandro Prada[a,]*, Elena Bee[a], Maurizio Grigiante[a], Paolo Baggio[a]

[a]*Dep.of Civil, Environmental and Mechanical Engineering, University of Trento, via Mesiano 77, Trento 38123, Italy*

**Abstract**

The coming into force of the European Directive 2009/28/CE [1] increases the role of renewable energy sources to satisfy the energy consumptions of new buildings and major renovations. In this respect, the vapor-compression heat pump coupled with PV panels is a promising solution and, consequently, it is increasingly used for residential heating applications. This HVAC solution is especially advantageous in high performance building when low temperature hydronic systems are adopted. However, in these buildings some issues arise in the HVAC control and the building might be easily subject to poor comfort conditions when approaching the nZEB target while maintaining economical convenience. Besides, the seasonal performance of the heating system is strongly dependent on the HVAC design. Hence, the optimal size of the storage components is a key aspect in order to maximize the renewable coverage factor, overcoming the shift in time between PV production and energy demand. For this reason, different strategies may be adopted such as the thermal storage tank or the electricity storage in lead-acid battery.

This paper analyses the mix among the thermal storage tank, the lead-acid battery and the thermal capacitance of the building envelope for the optimal design solutions in three Italian climates. The complex interactions among building, occupants, weather conditions and HVAC systems are considered by means of a dynamic simulation tool. The optimal design solutions were studied, according to the cost optimal approach of the EPBD context, by means of a genetic algorithm developed in Matlab®. The energy performance for heating ($EP_h$) and the net present value (NPV) are considered as competitive goals.



Peer-review under responsibility of the scientific committee of the AiCARR 50th International Congress; Beyond NZEB Buildings.

*Keywords:* Heat Pump; Multi-Objective Optimization; Energy Storage; NZEB

* Corresponding author. Tel.: +39-0461-282516.
*E-mail address:* alessandro.prada@unitn.it

1876-6102 
Peer-review under responsibility of the scientific committee of the AiCARR 50th International Congress; Beyond NZEB Buildings
10.1016/j.egypro.2017.11.154

## 1. Introduction

Air-to-water heat pumps have an increasing share in the European heating market. According to the European Heat Pump Market and Statistics Report [2], they represent the fastest growing heat pump segment across Europe. This rapid increase in market share is partly linked to the performance improvements in the commercial products, both for nominal and part load conditions, due to the adoption of inverter-driven compressors. Additionally, the aerothermal energy source is considered a renewable source by the European Directive 2009/28/CE and, consequently, air-source heat pumps (ASHP) will have an important role in order to meet the mandatory provisions about the minimum coverage factor of renewable energy sources. In this respect, the ASHP coupled with PV panels is a promising solution and, consequently, it is increasingly used for residential heating applications.

However, it has been observed that some issues arise in the control of the HVAC systems due to the fast changes in energy demand. Consequently, the building might be easily subject to poor comfort conditions when the energy systems are installed in high performance houses which approach the nZEB target while maintaining economical convenience [3]. Additionally, the seasonal performance of the heating system is strongly dependent on the HVAC design, such as the components sizes (heat pump, water storage tank, PV battery), and on the adopted control strategy. Thus, an optimal concurrent design of the HVAC and control systems installed in high performance building is essential to ensure the reduction of energy consumption and the achievement of thermal comfort for the entire heating season [4]. For these reasons, energy storage systems play a key role in the correct integration of the HVAC systems in high performance buildings. In the residential sector, storage systems are used to shave the peak loads, to take advantage of the off-peak tariff and to increase the renewable coverage factor [5]. However, the primary role of these systems is to reduce the discrepancy between the source availability and the energy demand. Hence, energy storages will become essential in high performance buildings since both the energy demand and the renewable energy production are inherently intermittent.

**Nomenclature**

| | |
|---|---|
| Alt | Site Altitude [m] |
| $COP_{rated}$ | Full load rated coefficient of performance at 7/35°C [-] |
| $EP_h$ | Non-renewable part of the Energy performance for heating [kWh $m^{-2}$ $yr^{-1}$] |
| $HDD_{10}$ | Heating degree days on 10°C basis [K day] |
| $HDD_{18}$ | Heating degree days on 18°C basis [K day] |
| Lat | Latitude angle [deg] |
| Long | Longitude angle [deg] |
| IC | Initial cost [EUR] |
| NPV | Net Present Value based on 30 years lifespan [kEUR] |
| $n_{batt}$ | Number of lead-acid battery in series [-] |
| $n_{str}$ | Number of strings of 3 PV modules in series [-] |
| $Q_{batt}$ | Capacity of a single lead-acid battery [kWh |
| $SB_{start}$ | Starting hour of setback adjustment [h] |
| $SB_{stop}$ | Stopping hour of setback adjustment [h] |
| SHGC | Solar heat gain coefficient [-] |
| $T_{sb}$ | Temperature of setback [°C] |
| U | Thermal transmittance [W $m^{-2}$ $K^{-1}$] |
| $V_{stor}$ | Volume of the storage tank [liter] |
| *WFR* | Window to Floor ratio [-] |
| $\Phi_{rated}$ | Rated ASHP thermal output at 7/35°C [kW] |
| $\kappa_m$ | Areal heat capacity according to [26] [kJ $m^{-2}$ $K^{-1}$] |

In the literature, several works dealt with the energy storage for building heating systems. In particular, three energy storage strategies are available for the heating system in a high performance building with an ASHP and PV panels. The most traditional solution, widespread in the historic buildings, is the sensible heat storage in the building envelope. Thermal energy is stored in the building envelope by taking advantage of the areal heat capacity ($\kappa_m$) of the internal side of the building components. The influence of the thermal mass on the energy consumption of a building has been recently studied in [6]. However, the adoption of a thermal energy storages (TES) is the most diffuse solution. These systems store the energy by using either the sensible heat, the phase change, the sorption or the chemical reactions [7]. The residential buildings use to a large extent the sensible heat storage [8-12] by means of water tank either as a fill storage or a stratified storage tank. Finally, the use of lead-acid battery to store the PV energy production is a solution adopted to take advantage of the off-peak tariff and to pursuit the increment of the renewable coverage factor. This type of solution is gaining importance with the spread of the generating systems that use electricity and because of the power grid management issues. In a recent work [13], the authors quantify up to 21% the increment of PV self-utilization due to the use of small battery systems.

This study presents an analysis on the mix among thermal storage tank, lead-acid battery and thermal capacitance of the building envelopes for the optimal design solutions in two Italian climates. A coupled simulation of the house and its heating system was set up in the TRNSYS simulation suite. The optimal design is studied following the cost optimal approach of the EPB directive by changing some building and HVAC parameters such as the volume of the storage tank, the number and capacity of the lead-acid batteries and the thermal capacitance of the building envelope. The trade-off solutions among the two different optimization objectives are evaluated by coupling the dynamic simulation tool with a genetic algorithm code developed in Matlab®. Following on from this point, the mix of the energy storage solutions of the Pareto front configuration is deeply investigated. The analysis is carried out on both well and poorly insulated buildings in three Italian climates (i.e. Trento, Roma and Palermo), with the purpose of considering the effect of different solar gains and heating season length.

## 2. Method

### *2.1. Simulation Layout*

A coupled simulation of the simplified reference building proposed in [14] and its heating system was set up in the TRNSYS simulation suite. The building is a semi-detached houses having 100 $m^2$ floor, 3 m internal height, façades oriented towards the main cardinal directions and a south window exposure (Fig. 1). An adiabatic boundary condition was imposed to the wall adjacent to the other building, while all the other surfaces are considered to be directly exposed to the external environment.

Two different values of the envelope characteristics were set in order to take into account both an existing and high performance building (Table 1). The linear thermal transmittances of thermal bridges were computed according to the EN ISO 10211 [15] by using the finite element approach. The infiltration rates were estimated according to the procedure presented in the standards EN 12207 [16] and EN 15242 [17] and the values are presented in (Table 1).

Table 1. Building characteristics.

| Variable | Units | Existing Building (EB) | High Performance Building (HPB) |
|---|---|---|---|
| $U_{wall}$, $U_{roof}$, $U_{floor}$ | W $m^{-2}$ $K^{-1}$ | 0.80 | 0.28 |
| $U_{glass}$ | W $m^{-2}$ $K^{-1}$ | 5.69 | 0.60 |
| $U_{frame}$ | W $m^{-2}$ $K^{-1}$ | 3.2 | 1.6 |
| SHGC | - | 0.81 | 0.34 |
| WFR | % | 19.9 | 19.9 |
| Infiltration Rate | ACH | 0.2 | 0.16 |

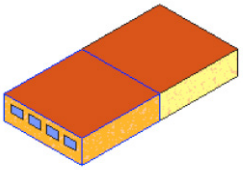

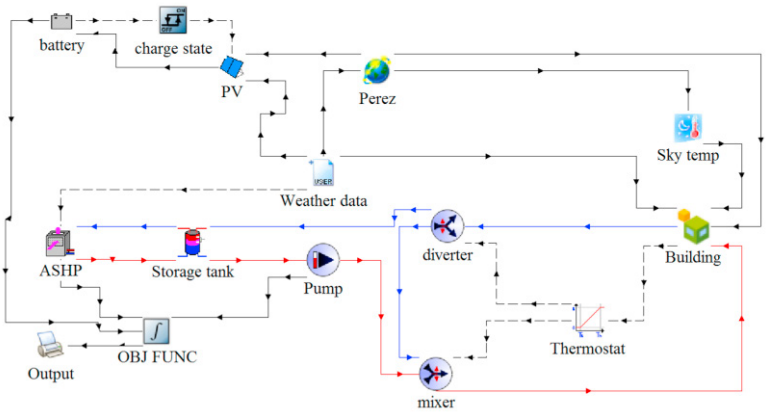


Fig. 1. Simplified reference building with south window exposure [14] and the TRNSYS simulation layout.

The heating system is based on an ASHP, with variable speed compressor, coupled with radiant floor panels. The radiant floor design is referred to a typical commercial configuration with PE−X pipes having a diameter of 0.016 m, a thickness of 0.002 m and a thermal conductivity of 0.44 W $m^{-1}$ $K^{-1}$. The supply temperature is adjusted according to an outdoor reset control while an ambient thermostat keeps the setpoint temperature to 20 °C during the occupied periods. On the contrary, the setback temperature ($T_{sb}$) and the time to setback start ($SB_{start}$) and stop ($SB_{stop}$) are optimization variables.

Standard and TESS libraries are used to model the building and HVAC systems, except for the ASHP. The part load behavior of an inverter ASHP is modeled by means of the new subroutine proposed in [18] described by a performance curve depending on the capacity ratio (CR) according to the EN 14285 [19]. The performance curve provides the ratio of the part load COP over the rated COP at full load and nominal conditions of sink and source temperatures. Two points fully identify the change in the ASHP operation at part-load. The first is the $CR_{deg}$ where the COP begins to degrade due to the on/off cycles while the second is the $CR_{max}$ value providing the CR corresponding to the maximum COP. An on/off controller with a dead-band turns the ASHP off when it reaches the lower modulating limit and water is warmed up more than required. The heating system is powered by either grid or photovoltaic (PV) electric power in an UPS like mode, thus avoiding the batteries operation in parallel with the grid. Hence, the system is connected to the grid only when the battery has been completely discharged. The simulations of the heating period were carried out considering the hourly weather data of three Italian cities having 4A and 3A climate according to the ASHRAE classification [20] (Table 2).

Table 2. Climate characteristics of the reference cities.

| City | Class | Lat. | Long. | Elev. | $HDD_{18}$ | $HDD_{10}$ |
|---|---|---|---|---|---|---|
| Trento | 4A | 46.023 N | 11.127 E | 185 | 2791 | 1029 |
| Roma | 3A | 41.921 N | 12.523 E | 32 | 1330 | 195 |
| Palermo | 3A | 38.131 N | 13.328 E | 50 | 1054 | 40 |

## *2.2. Genetic Algorithm (GA) implementation*

The genetic algorithm (GA) implemented in Matlab® is the Elitist Non-dominated sorting algorithms NSGA-II firstly proposed by Deb [21]. However, several customizations were introduced in the sampling, crossover, mutation, selection procedures and stopping criteria with the purpose of increasing the GA performances. For

instance, the random sampling of the population could lead to an over-focus on same regions of the hyperspace without sampling in others. Hence, the code was complemented with a Sobol sequence sampling in order to overcome the clustering which can occur with sample random sampling or quasi random generator. Sobol sequence is a low-discrepancy sequence, which aims to give a uniform distribution of values in higher dimensions.

Another customization deals with the selection of the best individuals that become the parents for the next generation. The Matlab® script implemented the tournament selection without replacement presented in [22]. A short list of four eligible parents are randomly chosen and the best individual out of that set to be a parent. Following on from this point, the code combines the genetic characteristics of both parents, giving rise to the new generation that is based on the arithmetic weighting of parents' genes. The 80% of the next generation is produced by the crossover and the remaining individuals in the next generation becomes from the population mutation. Mutation is applied at a random point in a random individual. In particular, a randomly selected gene is replaced by a uniformly distributed random value that meet the gene range. The hypervolume measure, originally proposed by Zitzler and Thiele [23], was used as a stopping criterion. Although the drawback of the higher computational cost, the maximization of this index is the necessary and sufficient condition for the Pareto optimal solutions of a discrete MOO problem as proved by Fleischer [24].

### *2.3. Genetic Algorithm (GA) Objectives*

The fitness function of the optimization algorithm is a Matlab® script that writes the input file and launches TRNSYS model for the energy simulation. After the model execution, the script reads the TRNSYS outputs and post-processes the simulation results in order to compute the two GA objectives.

The first objective index is the non-renewable part of the energy performance for heating ($EP_h$). This objective was calculated by summing for each time step the power withdraw from the grid required by the circulation pump and by the ASHP. This sum is then divided by the building floor area and multiplied by the primary energy conversion factor, i.e. 2.18 according to the Italian context.

The second GA objective is the net present value (NPV), calculated to quantify the economic benefits of each design solution. This approach allows the analysis of different time series of cash flows related to each solution based on a lifespan that was considered equal to 30 years. The NPV takes into account the initial investment cost, the annual running costs, the maintenance cost, the replacement costs, and the residual value, according to the standard EN 15459 [25].

The initial costs were defined starting from a market survey, by defining a pattern of costs as a function of the main product characteristics.

$$\begin{cases} IC_{ASHP} = COP_{rated}^{2.1305} \cdot \left(127.03 + 20.71 \cdot \Phi_{rated}\right) \\ IC_{stor} = 2.60 \cdot 10^{-3} \cdot V_{stor} + 456.4 \\ IC_{PV} = 1550 + 862.5 \cdot n_{str} \\ IC_{batt} = 0.274 \cdot Q_{batt}^{0.9376} \cdot n_{batt} \end{cases} \quad (1)$$

### *2.4. Optimization Variables*

Three different types of variables have to be optimized in order to improve the performance of heating system and to better design the coupling with the building. Firstly, the design variables affecting the HVAC performance have to be correctly designed by considering the specific characteristics of the building construction and operation. In this respect, the variables optimized in this work were the sizes of the main components such as ASHP, storage tank, PV modules and batteries (Table 3).

The other variables, not affecting the initial costs, are related to the building management. In this case the optimal orientation angles of the PV modules, the choice of the setback temperature and the setback schedules were considered.

Table 3. Optimization Variables.

| Variable | Units | Min | Max | Step |
|---|---|---|---|---|
| | HVAC sizes | | | |
| $V_{stor}$ | $m^3$ | 0.05 | 2.00 | 0.05 |
| $\Phi_{rated}$ | kW | 4 | 14 | 0.2 |
| $n_{str}$ | - | 1 | 8 | 1 |
| $Q_{batt}$ | Wh | 108 | 2376 | 108 |
| $n_{batt}$ | - | 1 | 6 | 1 |
| | HVAC management and adjustment | | | |
| PV azimuth | deg | East | West | 45 |
| $T_{sb}$ | °C | 10 | 20 | 1 |
| $SB_{start}$ | H | 7 PM | 11 PM | 0.5 |
| $SB_{stop}$ | H | 5 AM | 8 AM | 0.5 |
| | Building Design | | | |
| $\kappa_m$ | kJ $m^{-2}$ $K^{-1}$ | 30 | 200 | 1 |

Finally, the areal thermal capacitance of the building envelope was optimized with the purpose of understanding the optimal mix of energy storage among batteries, storage tank and building envelope (Table 3). The initial cost of the envelope was assumed constant and not dependent on the areal heat capacitance of the structure, as the material accounts for a limited share of the total construction cost.

## 3. Results

The results of the analyses are a series of Pareto fronts for each reference building showing the trade-offs between the two optimization goals. The frequency of each energy storage strategy in the Pareto optimal solutions has been analyzed by plotting the Pareto points with different colors according to the values of either the storage tank volume, the battery total capacity or the areal thermal capacitance of the opaque envelope (Fig. 2).

In each graph of the Fig. 2 the Pareto fronts are represented both for the existing building (EB top right) and for the high performance building (HPB bottom left). Fig 2 clearly shows how the shape of the Pareto fronts depends on the climate. Less harsh is the heating season and more tilted is the Pareto front. This is because the reduction of the non-renewable part of the energy performance for heating requires technical solutions whose initial costs have a greater payback time due to the low energy saving and, consequently, a greater NPV. Besides, a lesser distance between the Pareto fronts of EB and HPB is evident in less severe climates. The following paragraphs do a more extensive discussion on the optimal choice of energy storage solutions in the three climates.

### *3.1. Water storage tank*

The first set of graphs in Fig. 2 shows the storage tank volume in the Pareto front solutions for the three investigated locations. The points with high $EP_h$ are those with smaller storage tank both for the EB and the HPB in all the investigate climates. Thus the choice of a smaller buffer storage rewards the economic aspect thanks to the lower initial cost. On the other hand, the small storage tank allows to use less PV energy production and it induces the ASHP to operate at a lower part load ratio with an increasing number of on/off during the duty cycles.

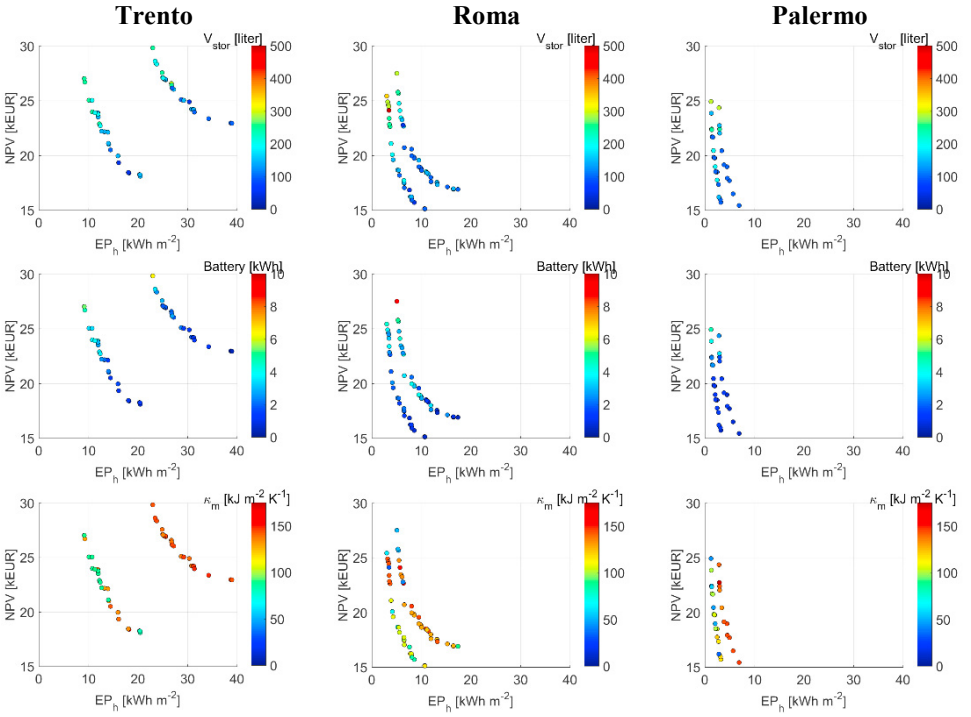


Fig. 2. Energy storage strategies in the Pareto front solutions for the three climates.

This results in a degradation of the value of the seasonal coefficient of performance (SCOP). Notice that the reduction of $EP_h$ obviously causes an increase in the NPV also because of the initial cost of the higher water tank of these solutions. This is more evident in Trento and Rome, and especially in HPB, where the optimal tank sizes come to reach the 300 liters. Only in a few cases, the optimal tank volume reaches the 500 liters since also the tank heat losses increase with increasing hot water storage volume. The trend of the distributions of the storage tank volumes in the optimal solutions is visible in Fig. 3. The graphs show the cumulative distribution function (CDF) for the existing buildings, in blue, and for the high performance buildings, in red. Notice that the red curve is shifted to the right compared to the dashed blue line for all the three locations. This indicates that there is a trend in the choice of storage tank with a greater volume in the HPB with respect to the EB.

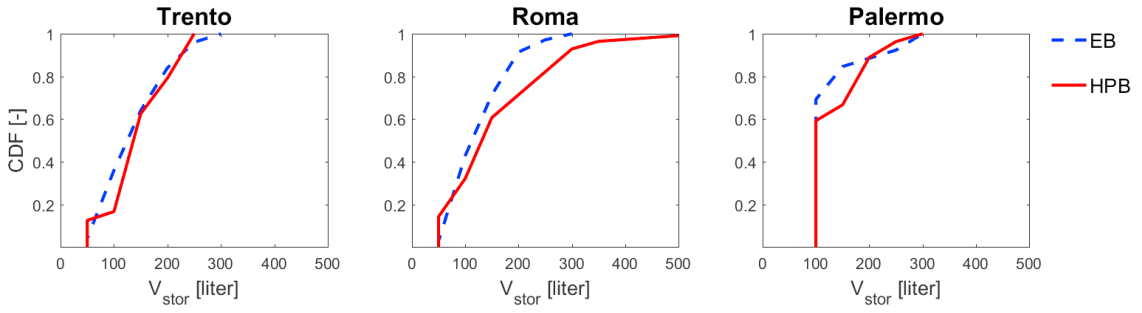


Fig. 3. Cumulative distribution function of the water storage volume in the Pareto solutions

The lower the insulation level of the opaque envelope, the lower the optimal storage tank volume. This is justified by the results shown in Fig. 5. As it happens in historical buildings, the envelope performance is mainly reached through the thermal capacitance of the structure in poorly insulated buildings. Thus the envelope capacitance can be exploited reducing the required volume of the water storage tank. This difference is hardly marked in Trento, where the curves are closer, but it is more evident in Palermo and especially in Rome. In HPB the optimum storage capacity comes up to 500 liters in Roma when smaller batteries and lightweight envelopes are used.

### *3.2. Battery total capacity*

The levels of total installed capacity of the lead-acid batteries in the optimal solutions are plotted in the second line of graphics in Fig. 2. The total battery capacity is computed as the product of the single battery capacity to the number of installed batteries.

As for the water storage tank, a prevalence of small battery capacities emerges for the solution with a greater $EP_h$ for all the three localities. This result shows how the required energy storage, can also be achieved with the envelope storage, thus minimizing the NPV both in EB and in HPB. Hence, small water storage tanks and low battery capacitance are required for these solutions. To further improve $EP_h$ however, the size of the batteries must be increased and, consequently, the value of the NPV grows. The energy optima are characterized by the maximum value of the battery capacity in all three cities. The maximum size of the lead-acid battery is roughly equal to 6 kWh in Trento and to 4.5 kWh in Palermo. Note that in Rome, there is a point characterized by a total capacity of about 10 kWh for the EB. This large battery capacity ensures the best energy performance for the EB case and it is installed in a poorly insulated building with a lightweight envelope.

The analysis of the cumulative distribution curves shows the conflicting trends in the three investigated climates analyzed. Firstly, the 60% of the Pareto solutions have an installed battery capacity lower than 4 kWh in Trento and Rome while, the size is reduced to less to 1 kWh in 60% of cases in the Mediterranean climate of Palermo, due to the reduced heating needs.

Comparing the two building insulation levels, there is a tendency to a greater battery capacity in HPB in Trento and in Palermo, whereas the contrary happens in Rome. This is because the HPB has generally lightweight envelope due to the increased insulation level of the walls. For this reason, the role of the energy storage in these buildings goes from the structure to the HVAC systems. Rome has an average daily radiation in the heating season greater than the other locations, also due to the different heating period length (Table 4). Hence, also the EB has a reduced need for solar gain storage because of the greater solar radiation and the south window exposure. Thus, the areal thermal capacitance becomes of the same magnitude of the HPB case (Fig. 5). Furthermore, for some configurations the HPB buildings require a greater thermal capacity of the structures to reduce the overheating phenomena

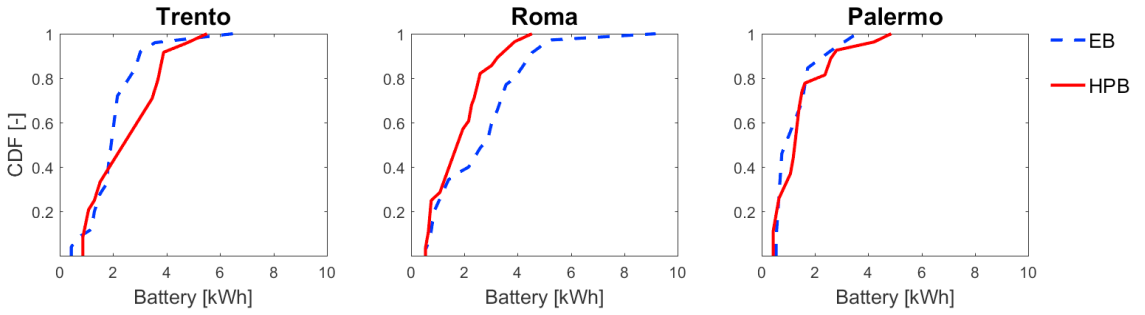


Fig. 4. Cumulative distribution function of the total battery capacitance in the Pareto solutions

Table 4. Climate variables during the heating season.

| Variable | Trento | Roma | Palermo |
|---|---|---|---|
| Dry Bulb Temperature [°C] | | | |
| Mean | 4.8 | 10.4 | 12.0 |
| Std. Deviation | 5.7 | 4.2 | 3.4 |
| Daily Global Horizontal Radiation [Wh m$^{-2}$] | | | |
| Mean | 1998 | 2605 | 2446 |
| Std. Deviation | 1372 | 1634 | 1218 |

### *3.3. Areal thermal capacitance of the envelope*

The last series of charts in Fig. 2 emphasizee the dependence of the optimal value of areal thermal capacitance on the insulation level. The higher the insulation level the lower the required thermal capacitance of the building envelope. For instance, the optimal $\kappa_m$ is roughly equal to 150 kJ K$^{-1}$ m$^{-2}$ for EB in Trento while it decreases to 90 kJ K$^{-1}$ m$^{-2}$ in case of HPB. However, this difference becomes less marked in less harsh climates such as Roma and Palermo. Additionally, the variability of $\kappa_m$ within each Pareto front increases in Roma and Palermo. While for Trento there are only two optimal $\kappa_m$ as a function of the insulation levels, multiple solutions exist in the other cities depending on the energy storage and on the management of the heating plant.

By analyzing the cumulative distribution functions, we note the different behavior of Roma as already mentioned in the previous sections. There is a significant distance between EB and HPB curves in the other two climates, especially for the lower values of $\kappa_m$. For example, the 20% of the front solutions have a value of $\kappa_m$ lower than 80 kJ K$^{-1}$ m$^{-2}$ and 140 kJ K$^{-1}$ m$^{-2}$ respectively for the cases HPB and EB in Trento and lower than 50 kJ K$^{-1}$ m$^{-2}$ and 140 kJ K$^{-1}$ m$^{-2}$ for the same cases in Palermo. On the contrary, the two CDF have the same value in Rome. The different behavior is due to the lower thermal capacitance of the case EB caused by the greater availability of solar gains.

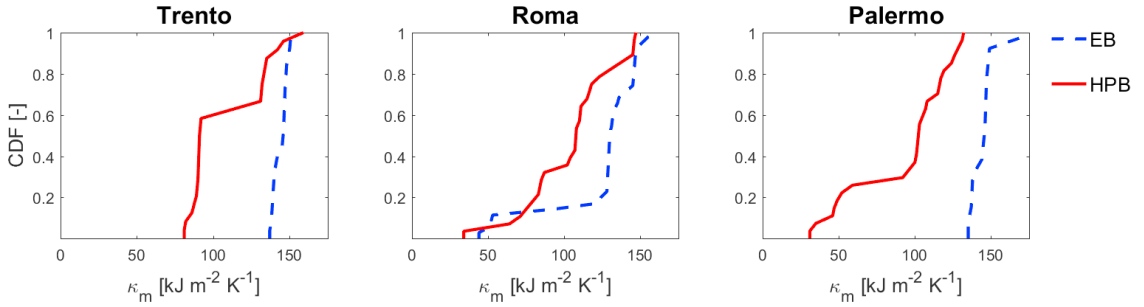


Fig. 5. Cumulative distribution function of the envelope areal capacitance in the Pareto solutions

## Conclusions

This work analyzed the optimal mix between the three different energy storage solutions during the heating season in a simplified reference building in three different Italian climates by means of a multi-objective optimization.

Firstly, the results show that the optimal thermal capacitance of the envelope depends on the building insulation level. In high-performance buildings with well-insulated walls, a lower thermal capacitance of the envelope is required to take advantage of the solar gains in the building energy balance. Hence, in well-insulated buildings the role of energy storage in the heating season passes from the building envelope to the HVAC systems.

Analyzing the volume distribution of the storage tank, the 60% of the solutions in the Pareto front has a volume lower than 150 liters in Trento and Rome while in Palermo the 0.6 fractile is equal to 100 liters. Similarly, the total battery capacity is less than 2 kWh in Trento and Rome and less than 1 kWh in Palermo for the 60% of the optimal solutions. However, in order to achieve the best energy performance, higher tank volumes and battery capacity are required in order to ensure a greater renewable coverage factor. The results thus show that in 99% of the optimal solution there are a volume lower than about 300 liters in the three localities and battery capacitances lower than 5 kWh in Trento and Rome and lower than 3.8 kWh in Palermo. Therefore, the transition from the 0.6 fractile to the 0.99 fractile implies an increasing of the tank volume of about two times in Trento and Rome and three times in Palermo whereas the increment of the battery capacity rises to 2.5 times in Trento and Rome and about four times in Palermo.

## Acknowledgements

This study has been performed in the frame of the NZEBnet project. The research leading to these results has received funding from the Italian Ministry for Education, University and Research through the PRIN2015 program.

## References

[1] European Parliament. Directive 2009/28/EC of The European Parliament and of the Council of 23 April 2009 on the promotion of the use of energy from renewable sources and amending and subsequently repealing Directives 2001/77/EC and 2003/30/EC. Official Journal of the European Union. 2009.
[2] EHPA. European Heat Pump Market and Statistics Report 2015. EHPA, European Heat Pump Association 2015.
[3] Penna P., Prada A., Cappelletti F., Gasparella A.. Multi-objectives optimization of energy efficiency measures in existing buildings. Energy and Buildings, 2015, 95:57 – 69, 2015
[4] Carlon E., Schwarz M., Prada A., Golicza L., Verma V.K., Baratieri M., Gasparella A., Haslinger W., Schmidl C. On-site monitoring and dynamic simulation of a low energy house heated by a pellet boiler. Energy and Buildings, 2016, 116: 296-306
[5] Belz K., Kuznik F., Werner K.F., Schmidt T. and Ruck W.K.L. Thermal energy storage systems for heating and hot water in residential building. In Woodhead Publishing Series in Energy, edited by Luisa F. Cabeza, Woodhead Publishing Pages 441-465, Advances in Thermal Energy Storage Systems 2015.
[6] Arcuri N., Carpino C., De Simone M. The role of the thermal mass in nZEB with different energy systems. Energy Procedia, 2016; 101:121-8
[7] Hadorn, J.C. Advanced storage concepts for active solar energy. In proceedings of EUROSUN 2008 – 1st Int. Cong. On Heating, Cooling and Buildings, Lisbon –Portugal 2008.
[8] Arteconi A., Hewitt N.J., Polonara F. Domestic demand-side management (DSM): Role of heat pumps and thermal energy storage (TES) systems. . Applied Thermal Engineering, 2013; 51:155-65
[9] Han Y.M., Wang R.Z., Dai Y.J. Thermal stratification within the water tank, Renewable Sustainable Energy Reviews, 2009; 13: 1014-26.
[10] Karim A. Experimental investigation of a stratified chilled-water thermal storage system. Applied Thermal Engineering, 2011; 31: 1853-60
[11] Pinel P., Cruickshank C.A., Beausoleil-Morrison I., Wills A. A review of available methods for seasonal storage of solar thermal energy in residential applications. Renewable and Sustainable Energy Reviews, 2011; 15(7): 3341–59
[12] Singh H., Saini R.P., Saini J.S. A review on packed bed solar energy storage systems. Renewable and Sustainable Energy Reviews, 2010; 14: 1059–69
[13] Kyritsisa A., Mathasa E., Antonucci D., Grottked M., Tselepisa S. Energy improvement of office buildings in Southern Europe. Energy and Buildings, 2016; 123: 17-33.
[14] Penna P., Prada A., Cappelletti F., Gasparella A. Multi-objective optimization for existing buildings retrofitting under government subsidization. Science and Technology for the Built Environment, 2015; 21: 847–61
[15] CEN. EN ISO 10211 Standard. Bruxelles: European Committee for Standardization. 2007
[16] CEN. EN 12207 Standard. Bruxelles: European Committee for Standardization. 1999
[17] CEN. EN 15242 Standard. Bruxelles: European Committee for Standardization. 2007
[18] Bee E., Prada A. and Baggio P. Variable-speed air to water heat pumps for residential buildings: evaluation of the performance in the Northern Italian climate. In CLIMA 2016 - proceedings of the 12th REHVA World Congress, vol. 3, Aalborg (Denmark), Aalborg University, Department of Civil Engineering. 2015.
[19] European Committee for Standardization. EN 14285 Standard. Bruxelles: European Committee for Standardization. 2012
[20] ASHRAE. Standard 196.Weather data for building design Standard climate zone. Atlanta. American Society of Heating, Refrigerating and Air-Conditioning Engineers, Inc. 2006
[21] Deb, K. A fast and elitist multi-objective genetic algorithm: NSGA-II. IEEE transactions on evolutionary computation 2002; 6: 182–197.
[22] Goldberg D. E., Korb B., Deb K. Messy genetic algorithms: motivation, analysis, and first results. Complex Systems 1989; 3: 493–530.

[23] Zitzler E., Thiele L. Multi objective evolutionary algorithms: A comparative case study and the strength pareto approach. IEEE Transactions on evolutionary computation 1999; 3: 257–71
[24] Fleischer M. The measure of pareto optimal applications to multi-objective metaheuristics. In EMO2003 proceedings of the 2nd International conference on Evolutionary Multi-Criterion Optimization, Faro, Portugal, 2003; 519–33.
[25] CEN. EN 15459 Standard. Bruxelles: European Committee for Standardization. 2007
[26] CEN. EN ISO 13786 Standard. Bruxelles: European Committee for Standardization. 2007